Jet suppression by accretion disk winds in the microquasar GRS 1915+105

Joseph Neilsen[1] & Julia C. Lee[1]

[1]*Harvard University Department of Astronomy, 60 Garden Street, MS-10, Cambridge, MA 02138*

Stellar-mass black holes with relativistic jets, also known as microquasars, mimic the behaviour of quasars and active galactic nuclei[1]. Because timescales around stellar-mass black holes are orders of magnitude smaller than those around more distant supermassive black holes, microquasars are ideal nearby 'laboratories' for studying the evolution of accretion disks and jet formation in black-hole systems[2]. Although studies of black holes have revealed a complex array of accretion activity, the mechanisms that trigger and suppress jet formation remain a mystery. Here we report the discovery of a broad emission line during periods of intense hard X-ray flux in the microquasar GRS 1915+105, and highly ionized narrow absorption lines during softer states. We argue that the broad emission line arises when the inner accretion disk is illuminated by hard X-rays, possibly from the jet[3]. In contrast, during softer states, when the jet is weak or absent[4], absorption lines appear as the powerful radiation field around the black hole drives a hot wind off the accretion disk[5−7]. Our analysis strongly suggests that this wind carries enough mass away from the disk to halt the flow of matter into the radio jet.

GRS 1915+105 is a 14 $M_\odot$ black hole accreting matter from a 0.8 $M_\odot$ K3 IV star in a wide 33.5-day orbit[8] (here $M_\odot$ is the solar mass). As the first known source of superluminal jets in the Galaxy[9], with a lightcurve exhibiting at least 14 distinct classes of high-amplitude variability due to rapid disk-jet interactions[3,10−15], this microquasar provides a fascinating example of the coupling between jets and accretion disks around black holes. To study this relationship, we have analysed archival HETGS[16] (High Energy Transmission Grating Spectrometer) observations of GRS 1915+105 from the Chandra X-ray Observatory. Between 2000 April 24 and 2007 August 14, the HETGS observed this mircroquasar 11 times with high spectral resolution, probing five of

the fourteen variability classes of this enigmatic X-ray source. The data include six observations of the faint, hard, jet-producing state[17] (Obs. H1–H6) and five observations of various bright, softer states (Obs. S1–S5).

As one of the brightest X-ray sources in the sky, GRS 1915+105 requires Chandra observations in a special high time-resolution mode to mitigate photon pileup (that is, two or more photons striking a single pixel during one CCD frame time). Unfortunately, this mode is not at present well calibrated, so it is currently impossible to fit a 'physical' model (e.g. a disk blackbody) to the broadband continuum. However, because we are mainly interested in spectral lines, we circumvent the calibration problems by fitting the X-ray continuum with a smooth 10th-order polynomial, revealing spectral features with widths less than 0.8 Å. The fraction of the 0.7–4.1 Å (3–18 keV) flux emitted below 1.4 Å (above 8.6 keV), which we call the hard flux fraction HF, clearly delineates the hard and soft states (see Fig. 1) and the observed spectral features (Fig. 2 and Supplementary Information). We will argue that these spectral differences are strong X-ray indicators of the disk-jet coupling in GRS 1915+105.

The states with high HF are dominated by a broad emission line near 1.86 Å (6.7 keV), which we tentatively identify as Fe XXV (Table 1). In contrast, strong narrow absorption lines near 1.77 Å (7.0 keV), consistent with Fe XXVI absorption blueshifted by $\sim 1,000$ km s^{-1}, are seen in softer states. In some cases, a weaker Fe XXV absorption line is seen at the same velocity. The absence of charge states other than hydrogen-like and helium-like iron in Obs. S2–S5 indicates a highly ionized absorber with ionization parameter $\xi = L_{\rm X}/nr^2$ of the order 10^4 (here $L_{\rm X}$ is the X-ray luminosity, n is the gas density, r is the distance from the source of ionizing radiation, and $\xi = 10^4$ corresponds to $T \sim 10^6$ K)[18]. These results are consistent with previous X-ray spectral studies of GRS 1915+105[19–21].

It has been postulated that the accretion disk is truncated at some distance from the black hole during the low hard state[3,22], when the spectrum may be dominated by hard X-rays from the corona or jet[4,23]. Coupled with infrared studies implicating jet activity in the production of emission lines

in GRS 1915+105[24], we conclude that the broad Fe XXV emission line is produced when the inner edge of the disk is illuminated by these hard X-rays. Our interpretation is substantiated by the fact that the equivalent width of the Fe XXV emission line increases with both $L_{\rm X}$ and the radio flux at 15 GHz as measured by the Ryle Telescope[15] (Fig. 3). Under the assumption that the line broadening ($\geq 12,500$ km s^{-1}) is due to orbital motion in a Keplerian disk, the line is emitted at $r \leq 1.1 \times 10^9$ cm ($\leq 255\ R_{\rm S}$, where $R_{\rm S}$ is the Schwarzschild radius of the black hole). This is a reasonable upper limit for the inner edge of the truncated disk.

In comparison, the inner edge of the accretion disk may lie much closer to the black hole (as little as $r = 3R_{\rm S}$ or less) during bright soft states[25]. In this context, we suggest that the absorption lines seen in GRS 1915+105 originate in an accretion disk wind. Several lines of evidence support this interpretation: the absorption lines (1) only appear during softer states, when the disk may be prominent and hard X-ray illumination is relatively weak (Fig. 4), (2) are all narrow and blueshifted (see Table 1), implying material flowing into our line of sight, and are accompanied by (3) a weak emission line at a slightly longer wavelength (Fig. 2). Together, (2) and (3) constitute a P-Cygni profile, a classic wind signature. Since a K-type companion cannot drive a strong wind, the wind must originate in the accretion disk. Furthermore, the wind speed corresponds to the escape velocity from the black hole at a distance of $r = 2.5 \times 10^{11}$ cm ($= 53460\ R_{\rm S}$), which is well inside the accretion disk of GRS 1915+105.

Given the high luminosity of this black hole binary and the strong variation of the equivalent width of the Fe XXVI absorption line with $L_{\rm X}$ (Table 1), it is likely that radiation pressure plays a role in driving this highly ionized wind[7]. However, radiation pressure alone (mainly imparted by ultraviolet emission lines) is inefficient at transferring momentum to a wind at $\xi > 10^3$ (ref 26). But at the high luminosity of GRS 1915+105, X-ray heating and thermal pressure can provide the extra boost to drive a hot, fast wind off the accretion disk for $r > 0.01 r_{\rm C}$, where the critical radius $r_{\rm C}$ is given by $r_{\rm C} = (9.8 \times 10^9) \times (M_{\rm BH}/M_\odot)/T_{\rm C8}$ cm. Here $M_{\rm BH}$ is the black-hole mass, and $T_{\rm C8}$ is the electron temperature in units of 10^8 K (refs 5,6). As our analysis indicates that the wind temperature $T_{\rm wind} \sim 10^6$ K, the wind could originate at any $r > 1.4 \times 10^{11}$ cm

($= 29340\ R_{\rm S}$). Although the relevant electron temperature could be much higher[5], this launching radius is consistent with our earlier estimate from the blueshift of the wind, so that thermal driving assisted by radiation pressure successfully explains the origin of this wind.

To estimate the mass loss rate from the wind, we fit the spectra with a photoionized absorption model that calculates the ionization balance for a shell of gas surrounding a central X-ray source[18]. This model is characterized mainly by the absorbing gas column density and ionization parameter $\xi \sim 10^4$; for a fixed luminosity and wind speed, a higher ionization parameter implies a smaller mass loss rate[19]. Assuming an accretion efficiency η, accretion rate $\dot{M}_{\rm acc}$, and wind covering factor f, our model implies a wind mass loss rate of $\dot{M}_{\rm W} = 188 \dot{M}_{\rm acc}\ \eta\ f$. With $f < 5\%$ (Fig. 2 legend) and $\eta = 6\%$ (ref 27), we calculate $\dot{M}_{\rm W} < 0.59\ \dot{M}_{\rm acc}$ ($\sim 10^{-8}$ M$_\odot$ yr^{-1}).

Interestingly, this wind drives approximately the same mass loss as the radio jet[17], suggesting that GRS 1915+105 is able to maintain a rough equilibrium between mass accretion and outflow, independent of its spectral state and the outflow mechanism, over the span of our observations. Furthermore, the noticeable decrease of HF with the equivalent width of the absorption lines (Fig. 4) indicates a complex competition between the accretion disk wind and the radio jet. When HF decreases, there are fewer hard X-rays available to over-ionize the wind, allowing it to carry away more of the matter that sustains the jet. Thus it appears that Comptonization and photoionization mediate the coupling between the jet and the disk in GRS 1915+105.

This is a strong indication that like their supermassive counterparts, stellar-mass black holes can regulate their accretion rate by feedback into their environments. More importantly, these observations clearly demonstrate that at sufficiently high luminosities in GRS 1915+105, the intense radiation field of the disk redirects the accretion flow, away from the radio jet and into a wind. By revealing a surprisingly simple jet-quenching mechanism in GRS 1915+105, our results point to fundamental new insights into the long-term disk-jet coupling around accreting black holes and hint at tantalizing evidence of the mechanism by which stellar-mass black holes regulate their own growth.

1. Mirabel, I. F. & Rodriguez, L. F. Sources of relativistic jets in the Galaxy. *Annu. Rev. Astron. Astrophys.* **37**, 409-443 (1999).

2. Fender, R. P. & Belloni, T. GRS 1915+105 and the disc-jet coupling in accreting black hole systems. *Annu. Rev. Astron. Astrophys.* **42**, 317-364 (2004).

3. Klein-Wolt, M., et al. Hard X-ray states and radio emission in GRS 1915+105. *Mon. Not. R. Astron. Soc.* **331**, 745-764 (2002).

4. Fender, R., et al. Quenching of the radio jet during the X-ray high state of GX 339-4. *Astrophys. J.* **519**, L165-L168 (1999).

5. Begelman, M. C., McKee, C. F., & Shields, G. A. Compton heated winds and coronae above accretion disks. I dynamics. *Astrophys. J.* **271**, 70-88 (1983).

6. Proga, D. & Kallman, T. R. On the role of the ultraviolet and X-ray radiation in driving a disk wind in X-ray binaries. *Astrophys. J.* **565**, 455-470 (2002).

7. Proga, D. Winds from accretion disks driven by radiation and magnetocentrifugal force. *Astrophys. J.* **538**, 684-690 (2000).

8. Greiner, J., Cuby, J. G., & McCaughrean, M. J. An unusually massive stellar black hole in the Galaxy. *Nature*, **414**, 522-524 (2001).

9. Mirabel, I. F. & Rodriguez, L. F. A superluminal source in the Galaxy. *Nature*, **371**, 46-48 (1994).

10. Belloni, T., Klein-Wolt, M., Mendez, M., van der Klis, M., & van Paradijs, J. A model-independent analysis of the variability of GRS 1915+105. *Astron. Astrophys.* **355**, 271-290 (2000).

11. Hannikainen, D. et al. Characterizing a new class of variability in GRS 1915+105 with simultaneous INTEGRAL/RXTE observations. *Astron. Astrophys.* **435**, 995-1004 (2005).

12. Mirabel, I. F. et al. Accretion instabilities and jet formation in GRS 1915+105. *Astron. Astrophys.* **330**, L9-L12 (1998).

13. Eikenberry, S. S., Matthews, K., Morgan, E. H., Remillard, R., & Nelson, R. W. Evidence for a disk-jet interaction in the microquasar GRS 1915+105. *Astrophys. J.* **494**, L61-L64 (1998).

14. Fender, R. P., Pooley, G. G., Brocksopp, C., & Newell, S. J. Rapid infrared flares in GRS 1915+105: evidence for infrared synchrotron emission. *Mon. Not. R. Astron. Soc.* **290**, L65-L69 (1997).

15. Pooley, G. G., & Fender, R. P. The variable radio emission from GRS 1915+105. *Mon. Not. R. Astron. Soc.* **292**, 925-933 (1997).

16. Canizares, C., et al. The Chandra high-energy transmission grating: design, fabrication, ground calibration, and 5 years in flight. *Pub. Astron. Soc. Pacif.* **117**, 1144-1171 (2005).

17. Dhawan, V., Mirabel, I. F., & Rodriguez, L. F. AU-scale synchrotron jets and superluminal ejecta in GRS 1915+105. *Astrophys. J.* **543**, 373-385 (2000).

18. Kallman, T. R. & Bautista, M. Photoionization and high-density gas. *Astrophys. J. Supp.* **133**, 221-253 (2001).

19. Lee, J.C., et al. High-resolution Chandra HETGS and Rossi X-Ray Timing Explorer observations of GRS 1915+105: a hot disk atmosphere and cold gas enriched in iron and silicon. *Astrophys. J.* **567**, 1102-1111 (2002).

20. Muno, M., Morgan, E. H., & Remillard, R. Quasi-periodic oscillations and spectral states in GRS 1915+105. *Astrophys. J.* **527**, 321-340 (1999).

21. Kotani, T., et al. ASCA observations of the absorption line features from the superluminal jet source GRS 1915+105. *Astrophys. J.* **539**, 413-423 (2000).

22. Esin, A. A., McClintock, J. E., & Narayan, R. Advection-dominated accretion and the spectral states of black hole X-ray binaries: application to Nova Muscae 1991. *Astrophys. J.* **489**, 865-889 (1997).

23. Markoff, S., Nowak, M. A., & Wilms, J. Going with the flow: can the base of jets subsume the role of compact accretion disk coronae? *Astrophys. J.* **635**, 1203-1216 (2005).

24. Eikenberry, S., et al. Spectroscopy of infrared flares from the microquasar GRS 1915+105. *Astrophys. J.* **506**, L31-L34 (1998).

25. McClintock, J., et al. The spin of the near-extreme Kerr black hole GRS 1915+105. *Astrophys. J.* **652**, 518-539 (2006).

26. Proga, D., Stone, J. M., & Kallman, T. R. Dynamics of line-driven winds in active galactic nuclei. *Astrophys. J.* **543**, 686-696 (2000).

27. Janiuk, A., Czerny, B., & Siemiginowska, A. Radiation pressure instability as a variability mechanism in the microquasar GRS 1915+105. *Astrophys. J.* **542**, L33-L36 (2000).

28. Houck, J. C. & Denicola, L. A. in *Astronomical Data Analysis Software and Systems IX* (eds Manset, N., Veillet, C. & Crabtree, D.) 591-594 (ASP Conference Series Vol. 216, 2000).

Supplementary Information is linked to the online version of the paper at www.nature.com/nature.

Acknowledgements We gratefully acknowledge support from the Harvard University Graduate School of Arts and Sciences (J. N.) and Faculty of Arts and Sciences (J.C.L.). We thank G. Pooley for providing the radio data used in this paper and we acknowledge conversations with R. Remillard, who provided the Rossi X-ray Timing Explorer spectra, and M. Begelman.

Author Contributions J.N. processed the data, performed spectral analysis, and wrote the paper. J.C.L. commented extensively on the manuscript. Both authors discussed the results at length.

Author Information Reprints and permissions information is available at npg.nature.com/reprintsandpermissions. The authors declare that they have no competing financial interests. Correspondence and requests for materials should be addressed to J.N. (jneilsen@cfa.harvard.edu).

Table 1: Spectral properties of GRS 1915+105

Obs. #	Obs. ID	X-Ray State[10]	L_{38}	HF	$S_{15\ \mathrm{GHz}}$ (mJy)	Line ID	λ_0 (Å)	λ_{obs} (Å)	Δv (km s^{-1})	W_0 (eV)	σ (km s^{-1})
S1	7485	ϕ	3.1	0.14	$\cdots$	Fe XXVI	1.7807	$1.7774^{+0.0004}_{-0.0005}$	-560^{+70}_{-80}	$-29.9^{+1.3}_{-1.6}$	650^{+150}_{-160}
S2	6581	γ	12.8	0.18	5 ± 3	Fe XXVI	1.7807	1.775 ± 0.001	-1000^{+240}_{-220}	$-21.9^{+2.2}_{-2.7}$	1160^{+280}_{-250}
S3	1945	ρ	4.9	0.21	3 ± 2	Fe XXVI	1.7807	1.772 ± 0.002	-1420^{+320}_{-310}	-7.2 ± 1.7	< 1120
S4	6580	β	5.9	0.21	20–60	Fe XXVI	1.7807	1.774 ± 0.002	-1100^{+360}_{-300}	$-19.3^{+3.2}_{-3.5}$	980^{+450}_{-420}
S5	6579	β	5.2	0.21	20–60	Fe XXVI	1.7807	$1.775^{+0.002}_{-0.003}$	-910^{+390}_{-430}	$-13.3^{+3.0}_{-2.9}$	< 1080
H1	660	χ	3.0	0.31	20 ± 4^{19}	Fe XXVI	1.7807	$1.775^{+0.004}_{-0.003}$	-910^{+630}_{-570}	$-4.8^{+1.6}_{-2.5}$	< 1300
H1	660	χ	3.0	0.31	20 ± 4^{19}	Fe XXV	1.868	1.89 ± 0.02	2830^{+3830}_{-3840}	53.0 ± 7.9	17820^{+2000}_{-2950}
H2	4587	χ	3.9	0.32	89 ± 8	Fe XXV	1.868	1.865 ± 0.006	-460 ± 980	101.1 ± 6.4	11120^{+840}_{-750}
H3	1944	χ	3.1	0.32	29 ± 1	Fe XXV	1.868	1.867 ± 0.009	-260^{+1460}_{-1480}	81.9 ± 7.1	12210^{+1290}_{-1100}
H4	4589	χ	3.6	0.33	80 ± 1	Fe XXV	1.868	1.861 ± 0.007	-1230^{+1180}_{-1150}	91.8 ± 6.9	11130^{+1110}_{-960}
H5	1946	χ	3.0	0.34	10 ± 3	Fe XXV	1.868	$1.86^{+0.01}_{-0.02}$	-2000^{+2300}_{-2340}	53.6 ± 7.4	11950^{+1930}_{-1580}
H6	4588	χ	3.2	0.36	90 ± 3	Fe XXV	1.868	1.867 ± 0.008	-130^{+1230}_{-1240}	82.1 ± 6.8	10590^{+1080}_{-950}

The 11 HETGS observations are listed in order of increasing hard flux fraction with their *Chandra* observation ID numbers and relevant spectral properties. 'S' indicates a soft state and 'H' indicates a hard state. The Greek letters identify the observations with one of the 14 variability classes of this microquasar[10]. L_{38} is the 0.7-4.1 Å (3-18 keV) luminosity, measured with the Rossi X-ray Timing Explorer (RXTE), in units of 10^{38} ergs s^{-1}. HF is the hard flux fraction, defined as the ratio of the unabsorbed 0.7-1.4 Å (8.6–18 keV) to 0.7–4.1 Å (3–18 keV) continuum flux. $S_{15\ \mathrm{GHz}}$ is the radio flux at 15 GHz, measured by the Ryle Telescope[15]. The line ID is our identification of the strongest line; we detect Fe XXVI in absorption and Fe XXV in emission. λ_0 is the ion's laboratory wavelength and λ_{obs} is the observed wavelength. Δv is the corresponding Doppler velocity. W_0 is the line equivalent width, and σ is the line width. All errors correspond to 90% confidence limits. Because of its intermediate hard flux fraction, Obs. H1 exhibits both a weak broad emission line and a weak narrow absorption line.

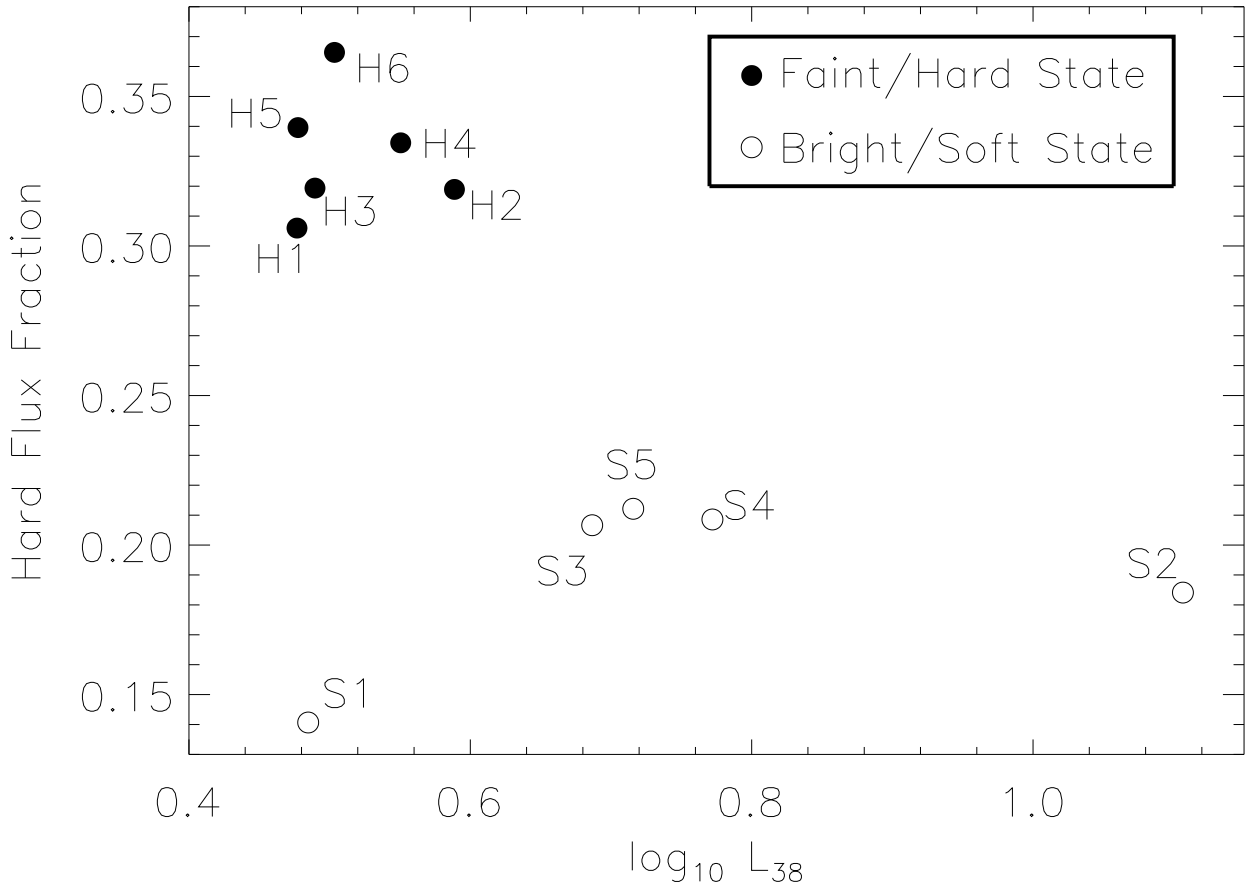

Figure 1 The X-ray luminosity and hard flux fraction for the 11 archival HETGS observations of GRS 1915+105. L_{38} is the X-ray luminosity in units of 10^{38} ergs s^{-1}, measured with RXTE from 0.7–4.1 Å (3–18 keV), assuming a distance of 12.5 kpc (ref 9) and neutral hydrogen absorption $(N_{\rm H} = 5 \times 10^{22}$ cm$^{-2})$[19] along the line of sight. The hard flux fraction, used as a proxy for the strength of the Comptonized emission from the corona or jet, is defined as the ratio of the unabsorbed continuum flux from 0.7–1.4 Å (8.6–18 keV) to 0.7–4.1 Å (3–18 keV). The 11 observations are classified as hard or soft based on previous X-ray studies[10]; as expected, the hard states have a higher hard flux fraction.

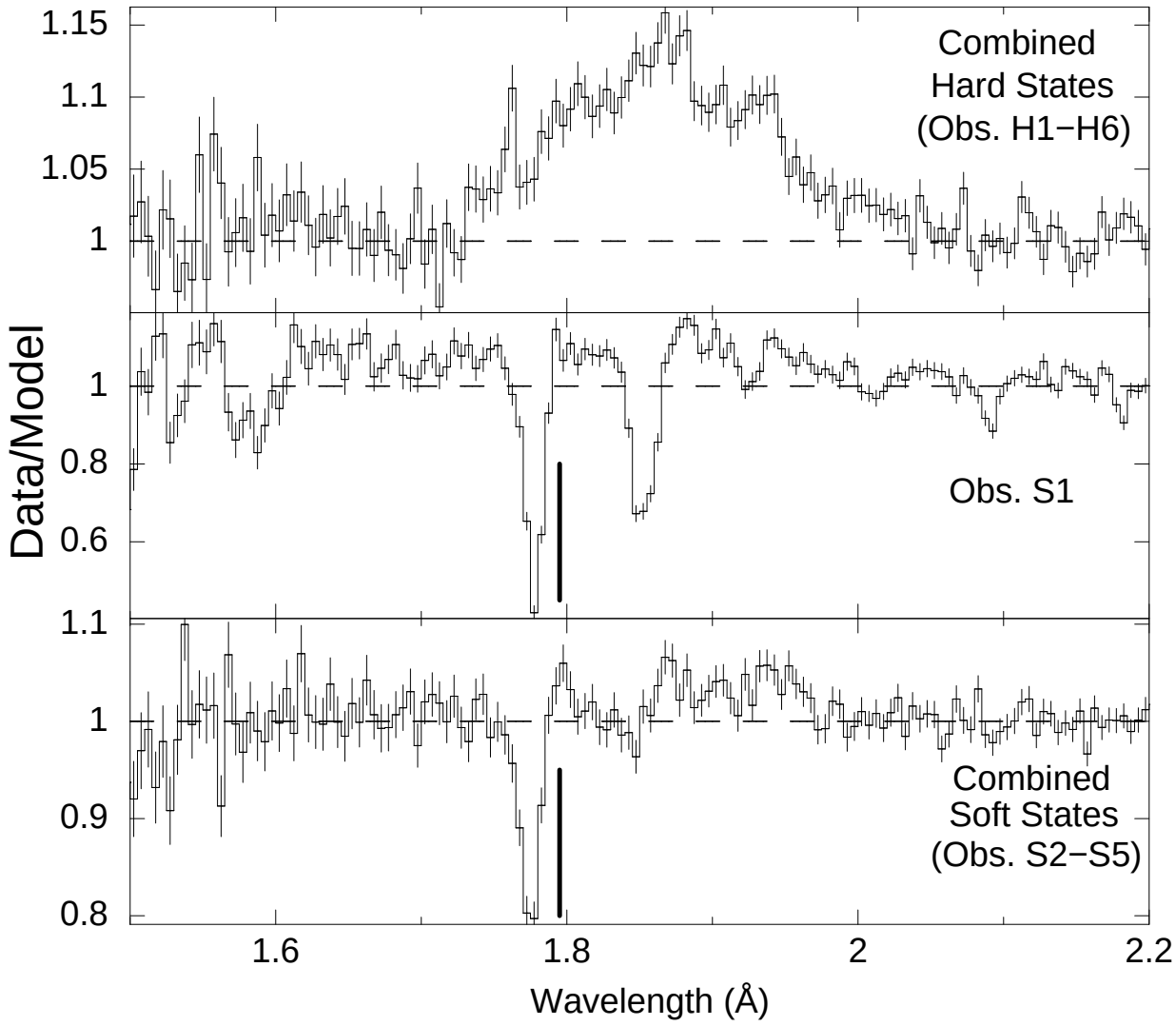

Figure 2 The data:model ratio for the continuum fits to the HETGS observations of GRS 1915+105. We plot the combined hard states (Obs. H1–H6) and combined soft states (S2–S5) for clarity; Obs. S1 is shown alone to highlight other strong lines. Plots of the individual spectra can be found in the Supplementary Information. The broad Fe XXV *emission* line distinguishes periods of significant hard X-ray illumination from softer states, which are dominated by strong Fe XXVI *absorption* lines. We use a simple Gaussian to measure the properties of the broad Fe XXV line (with the assumption that it is not a blend of emission from several Fe charge states) and find it has a line width $\geq 12,500$ km s^{-1}, much larger than the orbital velocity of either the companion star or the black hole[8]. We note that it represents a lower limit because our continuum-fitting procedure

would mask the red wing of any relativistically broadened emission line; the implied inner disk radius of $255\ R_{\rm S}$ is thus an upper limit. While the emission line width probes the size of the disk, the P-Cygni profile of the absorption lines constrains the geometry of the accretion disk wind. The vertical line indicates the position of the weak P-Cygni emission component. Because this emission component is weak, the wind must be confined to the equatorial plane of the disk. As the binary is viewed at an inclination $i = 70^\circ$ (ref 9), we can suppose that $i < 20^\circ$ above the midplane of the disk is a reasonable estimate (implying $f < 5\%$). Spectral analysis was performed with the ISIS[28] spectral fitting package. The errors shown are 68% confidence limits on the data:model ratio.

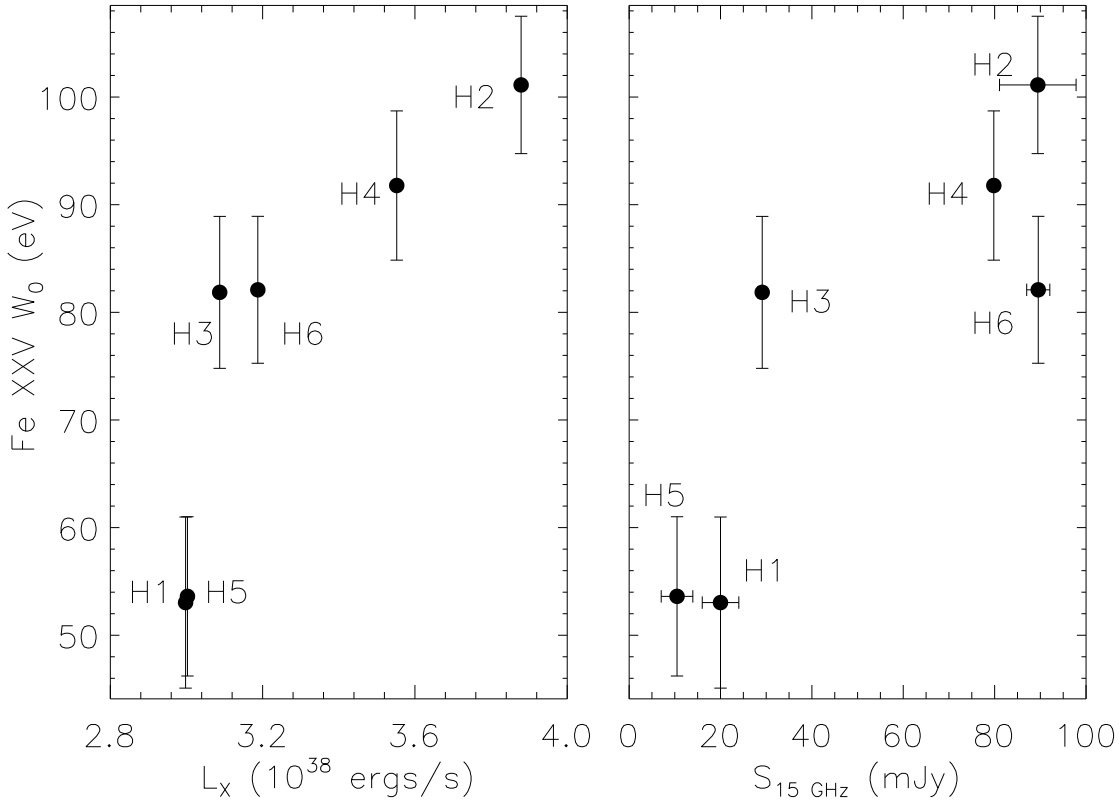

Figure 3 The equivalent width W_0 of the broad Fe XXV emission line in the hard states of GRS 1915+105 as a function of $L_{\rm X}$ (left) and radio flux (right). Because the emission line equivalent width is correlated with both $L_{\rm X}$ and $S_{15\ \rm GHz}$, it is more likely that the accretion disk is illuminated by the X-ray emitting base of the radio jet than by a hot, tenuous

corona. Because the hard flux fraction does not obviously scale with $L_{\rm X}$, more detailed studies are required to determine the complex relationship between the X-ray illumination that causes the broad lines and the hard X-rays that ionize the wind. W_0 was measured based on simple Gaussian fits; the actual values will be larger if continuum uncertainties have masked the broad red wing of the line. Errors shown for W_0 correspond to 90% confidence limits on the emission line flux; errors shown for the radio flux at 15 GHz ($S_{15\ \rm GHz}$; ref 15) are also 90% confidence limits.

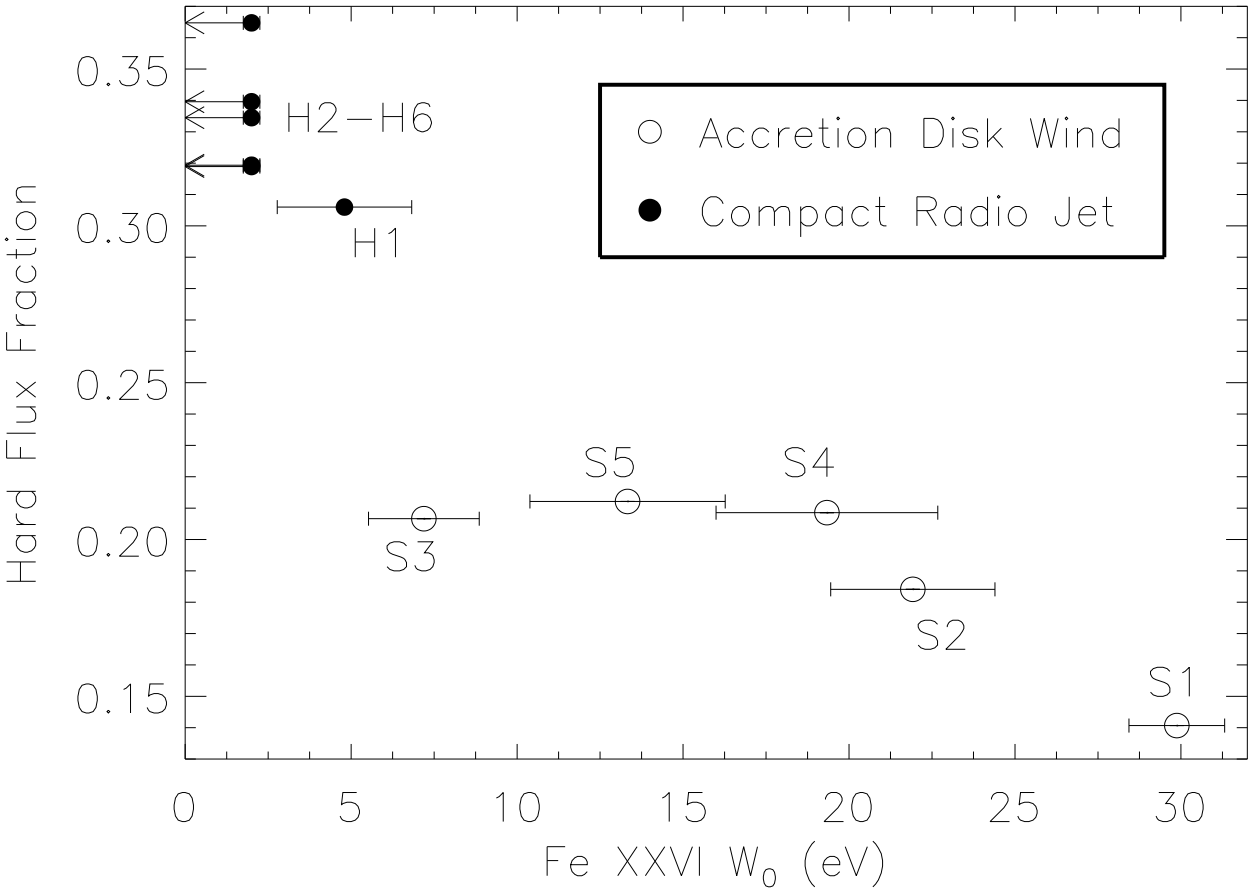

Figure 4 The hard flux fraction and the equivalent width W_0 of the Fe XXVI absorption line seen in GRS 1915+105. The hard flux fraction is defined as the ratio of the unabsorbed 0.7–1.4 Å (8.6–18 keV) to 0.7–4.1 Å (3–18 keV) continuum fluxes, measured with RXTE. This figure shows HF decreasing with W_0, implying that the jet weakens as the wind strength increases (and vice-versa). It appears that by carrying a significant amount

of matter away from the accretion disk, strong winds can suppress jet production. This figure illustrates the nature of the complex competition between the wind and the jet, because the trend can also be understood in terms of the hard X-ray illumination of the wind. In the hardest states, the corona/jet may completely photoionize the wind, so that the gas is transparent, and therefore the absorption lines are weak or absent and the mass loss rate in the wind decreases significantly. This effect can also explain (for higher hard flux fraction) the disappearance of the lower-ionization absorption lines present in Obs. S1. Because of the complicated coupling between the disk and jet, we do not rule out broadened emission lines in softer states, or narrow absorption lines in harder states. In fact, the presence of both a broad emission *and* narrow absorption lines in Obs. H1 provides further evidence of active competition between the wind and the jet. These results imply that HF is a viable indicator of accretion physics around black holes. The errors shown for the equivalent width correspond to 90% confidence limits on the absorbed line flux.

Supplementary Figure 1

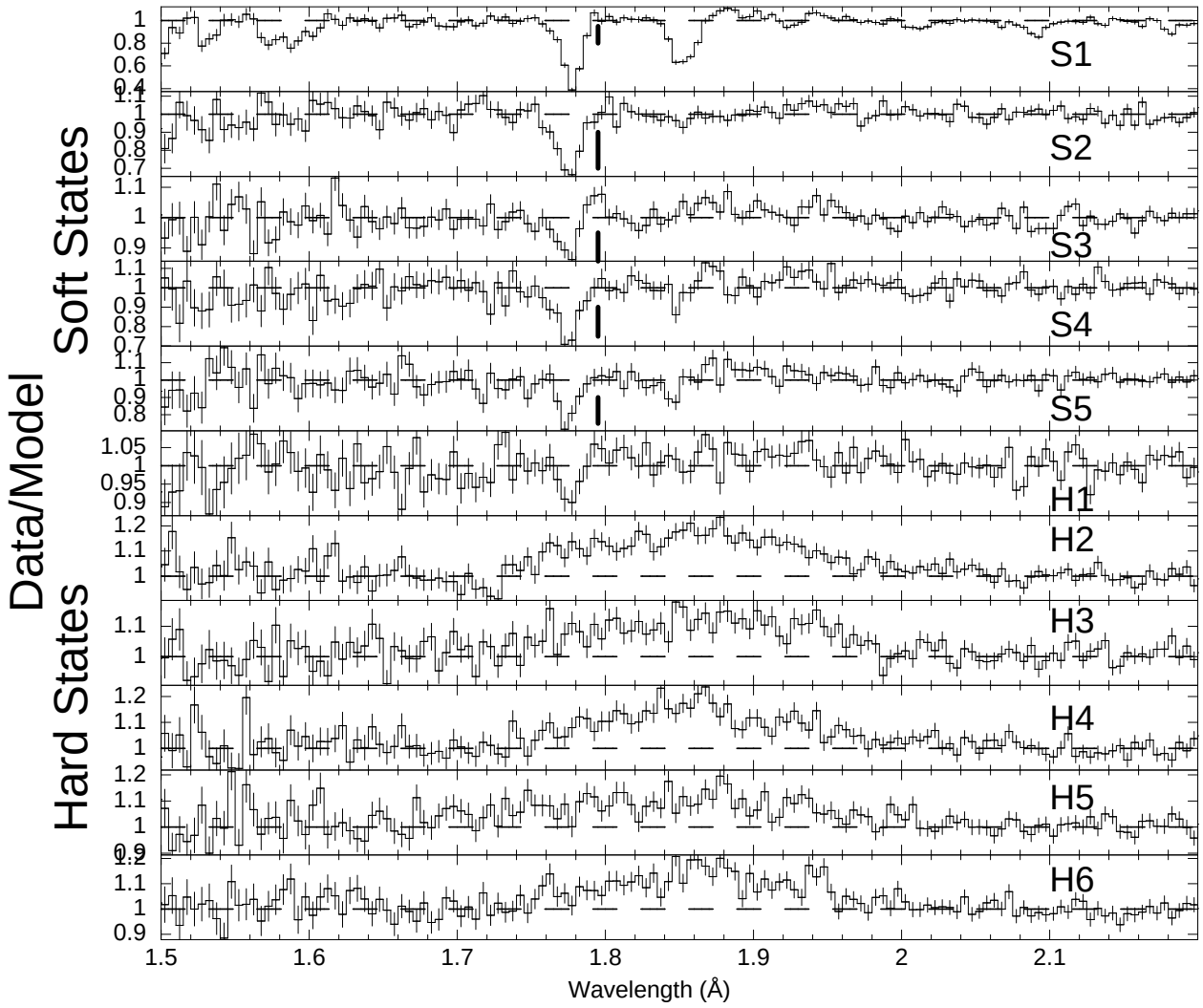

Figure 5 Data:model ratio for all 11 HETGS observations of the microquasar GRS 1915+105. The spectra are plotted in order of increasing hard flux fraction (the ratio of the unabsorbed luminosity in the 8.6–18 keV band and the 3–18 keV band). 'S' indicates a soft state and 'H' indicates a hard state. The error bars shown are 1σ statistical uncertainties on the data:model ratio. The vertical lines indicate the location of the emission component of the P-Cygni profiles.